JOURNAL OF APPLIED ELECTROCHEMISTRY 5 (1975) 351–358

Mössbauer spectroscopy investigation of the iron electrode during cycling in alkaline solution

Y. GERONOV

Central Laboratory for Electrochemical Power Sources, Bulgarian Academy of Sciences, Sofia, Bulgaria

T. TOMOV, S. GEORGIEV

Institute of Nuclear Physics, Bulgarian Academy of Sciences, Sofia, Bulgaria

Received 9 December 1974; revised 20 February 1975

The processes which take place in the iron electrode during cycling in alkaline solution were investigated by Mössbauer spectroscopy and the reaction products were determined quantitatively.

It was proved that β-FeOOH is invariably formed at the end of the second anodic reaction in 5 N KOH. At the end of charging there is always a certain amount of residual $Fe(OH)_2$.

After three to five cycles in 5 N KOH containing 9 $g\,l^{-1}$ LiOH, β-FeOOH is converted into Fe_3O_4. At the same time a drop is observed in the capacity of the electrode. At the end of charging under these conditions a certain amount of Fe_3O_4 was always found.

1. Introduction

The behaviour of the iron electrode in alkaline media has been repeatedly investigated [1–16]. However, in spite of the long history of these studies which extend over a period of more than fifty years, there is still no unity of opinions as to the nature of the oxidation products which form during the second anodic process and as to the mechanism which causes the arrest of the anodic processes.

X-ray diffraction analysis [5–7] yields some information on the electrochemical reaction products, but, owing to certain unavoidable experimental limitations, no quantitative data have been obtained; for example, the penetration depth of X-rays in the sample is comparatively small, sensitivity and precision are insufficient, etc. The recently applied magnetometric method [8, 9] yields only indirect and ambiguous information on the phases present in the electrode.

In a previous work [17] it was proved that Mössbauer spectroscopy is particularly appropriate for quantitative investigation of the iron electrode *in situ*. In the present work an iron electrode with a composition as close as possible to commercial electrodes was investigated. In addition, an attempt was made to obtain quantitative data for the reaction products obtained during cycling.

2. Experimental

All possible analytical applications of Mössbauer spectroscopy rely on one basic fact: the individual iron compounds (provided the Mössbauer isotope Fe^{57} is used) yield characteristic spectra which are usually sufficient for 'fingerprint' identification.

Quantitative Mössbauer analyses may be performed by taking into account the relationship between the number of iron nuclei bonded in a given phase and the peak intensities in the corresponding Mössbauer spectrum. We can write for the peak area of a given phase:

$$S = \phi.A.F_1(T_a) \qquad (1)$$

where $T_a = n\sigma_0 f'$. In this expression ϕ is a coefficient which accounts for the non-resonance atomic absorption in the sample, A is a coefficient which depends on the source used, n is the number of Fe^{57} nuclei per cm^2 of the sample bonded in a given phase, σ_0 is the resonance absorption cross-section, f' is a solid-state parameter (the Debye-Waller factor), typical for every phase, and T_a is called effective thickness.

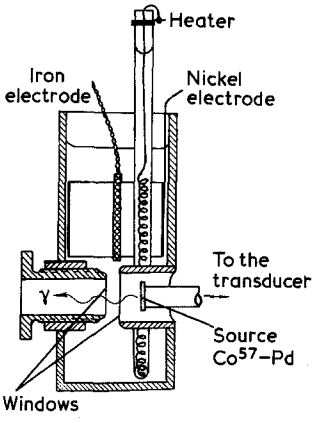

Fig. 1. Experimental cell.

The problem is considerably simplified if the individual phases are determined relatively. Then the peak area ratio for any two given phases may be written as:

$$\frac{S_1}{S_2} = \frac{F_1(T_{a_1})}{F_2(T_{a_2})}. \qquad (2)$$

In this case there is no need to determine ϕ and A, which is rather difficult. By means of appropriately selected standards one can plot calibration curves and carry out the desired quantitative determinations.

When the Mössbauer effect is used in a transmission geometry (the gamma-quanta of the source passing through the sample), the iron electrodes under investigation should be sufficiently thin. For the present study of electrodes of the following composition were prepared: 80% iron powder with a high iron content, 10% acetylene black, 5% polyisobutylene, and 5% iron wool [10]. The material was compressed at 0·5 T per cm^2 onto a nickel screen with 5 mesh per cm^2 and a wire diameter of 0·5 mm. The electrodes were rectangular with a geometric area of 5 cm^2 and a surface density (without the nickel screen) of about 25 mg cm^{-2}. In this way the electrodes had a sufficient mechanical rigidity at the expense of a somewhat lower current efficiency.

The electrodes were cycled in the upper part of a Lucite cell (Fig. 1). A nickel cylinder served as counter-electrode. The lower part of the cell was provided with two thin (0·1 mm) Lucite windows. The distance between the latter could be controlled. A heating element was mounted in the cell,

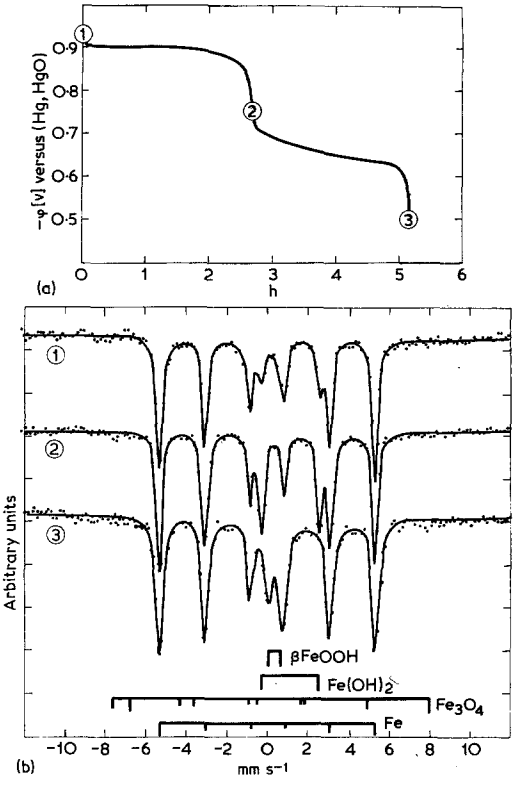

Fig. 2. (a) Discharge curve of an iron electrode in 5 N KOH at a current of 7 mA and at 30°C; (b) Mössbauer spectra of the same electrode recorded at points 1, 2 and 3 of the discharge curve.

thus making it possible to maintain the electrolyte temperature constant within ±0·5°C. During the determination of the Mössbauer spectrum the electrode was slid down and pressed between the windows in order to depress the non-resonance absorption in the electrolyte.

The Mössbauer source was moved by a velocity generator according to a linearly changing velocity law. The pulses detected by a gas-filled (argon-methane) proportional counter were amplified, discriminated and recorded in a multichannel analyser operating in a multiscaling mode. During the determination of the spectrum the cell circuit was opened. As shown by control measurements the phase composition of the electrode did not change within 1/2–1 h, which was the time required for determination of the spectrum.

The cycling conditions were: a 6–8 h charge at 8 mA and a discharge at 7 mA down to 0·5 V (vs Hg/HgO) at 30°C. Cycling was performed by means of a galvanostat.

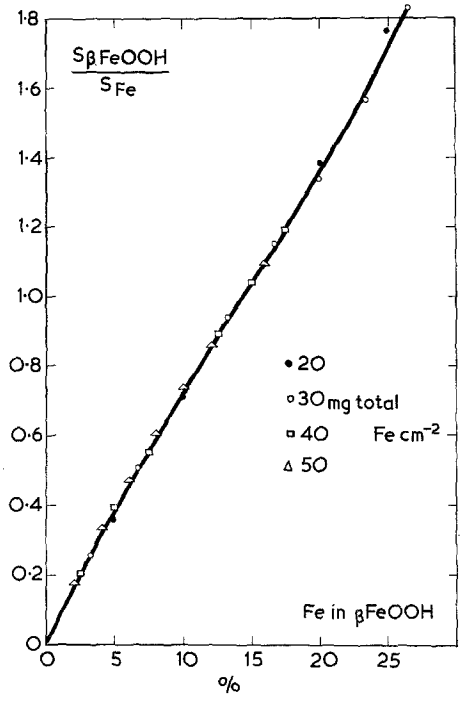

Fig. 3. Calibration curve. Ratio between the peak areas at 0·04 mm s^{-1} of β-FeOOH and 0·84 mm s^{-1} of metallic iron versus the amount of iron bonded as β-FeOOH as a percentage of the total iron in the electrode.

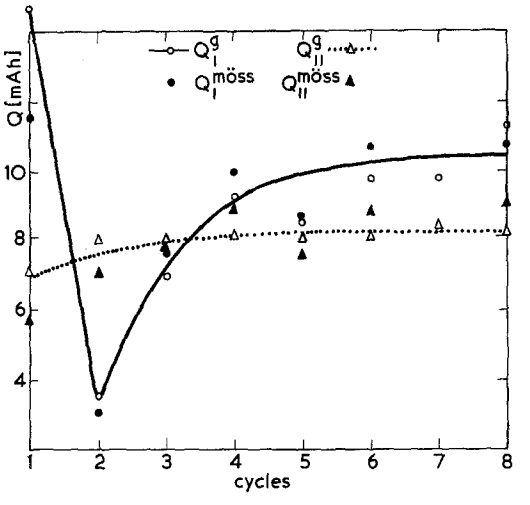

Fig. 4. Change in capacity during the first and second anodic processes during operation of the electrode in 5 N KOH. Q_I^g and Q_{II}^g are experimentally determined from the discharge curves, $Q_I^{möss}$ and $Q_{II}^{möss}$ are calculated from the quantitative phase analysis.

3. Experimental results

3.1. Electrochemical processes in a 5 N KOH electrolyte

3.1.1. Anodic process. Fig. 2 illustrates a typical discharge curve in 5 N KOH. The beginning of the discharge (−0·9 V), the end of the first anodic process (−0·75 V) and the end of the second anodic process (−0·5 V) are denoted by 1, 2 and 3, respectively. (Fig. 2)

Fig. 2 also shows the Mössbauer spectra recorded at points 1, 2 and 3, as well as the bar diagrams of the possible phases present. The centroid of the α-Fe spectrum was selected as the zero of the velocity scale.

The identification of metallic iron and of ferrous hydroxide is straightforward. The only doublet which cannot be unambiguously ascribed is that at 0·04 and 0·66 mm s^{-1} in the spectrum recorded at point 3. The two peaks might belong either to β- or γ-FeOOH since the parameters of these two phases are very close. In order to eliminate this uncertainty the spectrum of a discharged electrode was determined at 120 K. At room temperature the two polymorphs of FeOOH are paramagnetic and have different Néel temperatures — 295 and 77 K, respectively. In the recorded spectrum the doublet changes to a six-line pattern. This is typical for ferromagnetic states. The results obtained coincide with those reported by other authors [18] and indubitably show that the discharge iron electrode contains substantial amounts of β-FeOOH.

Thus the following phases were found during the anodic oxidation process of the iron electrode in 5 N KOH: in a charged state Fe and $Fe(OH)_2$ (in all cases except after the first charge) and in all cases at the end of the first anodic step; Fe and β-FeOOH (invariably at the end of the second anodic step).

A S_β/S_{Fe} calibration curve was plotted as a function of the percentage of iron present as β-FeOOH, under the assumption that the total iron content remains constant (such as is the case in a working electrode). It is seen that, up to 25%, the curve depends only weakly on the total iron content (Fig. 3).

No calibration curve was plotted for the determination of the amount of $Fe(OH)_2$ because of the difficulties connected with the preparation of this compound in a dry state. It was assumed that f' from Equations 1 and 2 has the same value for $Fe(OH)_2$ and β-FeOOH. The calibration curve

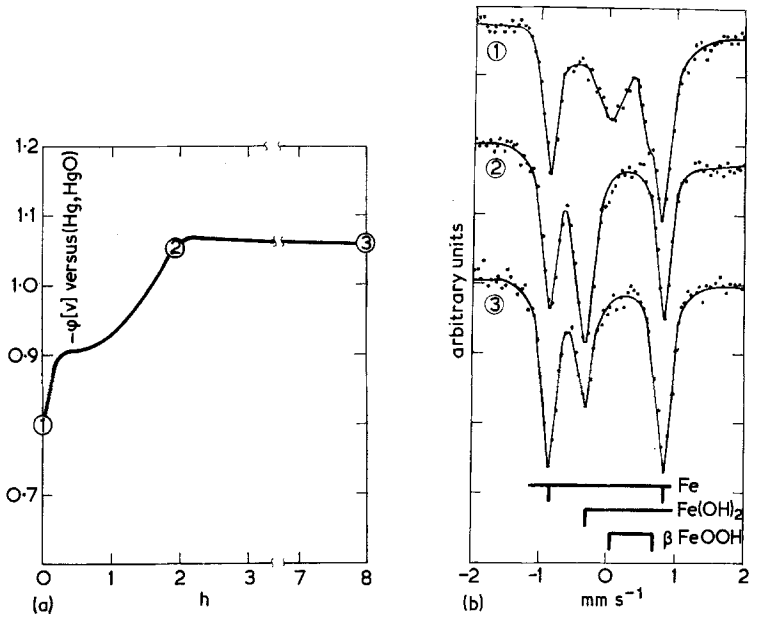

Fig. 5. (a) Charging curve of an iron electrode in 5 N KOH at a current of 8 mA and at 20°C; (b) Mössbauer spectra of the same electrode recorded at points 1, 2 and 3 of the charging curve.

from Fig. 3 was therefore used. The correctness of this assumption was confirmed by comparing the capacities of the electrodes investigated in the first anodic step, as shown later.

In order to save time the spectra were determined within the ± 2 mm s^{-1} range only. It is seen from Fig. 2 that in this range the three phases are immediately apparent. The spectra were treated either by cutting and weighing the curves or by the least-squares method using computer techniques [19] when a greater precision was required.

By this method the amounts of iron in every phase were calculated as percentages of the total iron for the characteristic points of the discharge curves. This, in turn, made it possible to calculate the charge for the first and the second anodic processes ($Q_{\mathrm{I}}^{\mathrm{möss}}$ and $Q_{\mathrm{II}}^{\mathrm{möss}}$). The experimental values were compared with those found from the discharge galvanostatic curves ($Q_{\mathrm{I}}^{\mathrm{g}}$ and $Q_{\mathrm{II}}^{\mathrm{g}}$).

Fig. 4 illustrates the results obtained for the entire formation process of an iron electrode in 5 N KOH. It is seen that the coincidence between $Q^{\mathrm{möss}}$ and Q^{g} for the two anodic processes is satisfactory. The discrepancies lie within the limits of the error in the quantitative determination of the individual phases (5–10%). (Fig. 4)

3.1.2. Cathodic process. Fig. 5 shows a typical charge curve and the Mössbauer spectra at points 1, 2 and 3 (1 is the start of the charge process, 2 is the end of the first cathodic process and 3 is the end of charge). It is apparent that at point 2 β-FeOOH is completely converted into $Fe(OH)_2$. At the same time the potential does not change any more and metallic iron formation as well as hydrogen evolution begin. At point 3 a certain amount of $Fe(OH)_2$ remains unchanged. This residual $Fe(OH)_2$ cannot be reduced even after a prolonged charging. (Fig. 5)

Table 1 illustrates the quantitative changes during the cathodic process in 5 N KOH. The calculations were similar to those performed for the anodic process, where $\Delta = (Q^{\mathrm{g}} - Q^{\mathrm{möss}}/Q^{\mathrm{g}})(100)$.*

In the following discharge $Q_{\mathrm{I}}^{\mathrm{g}} = 17$ mAh, which corresponds to the oxidation of 13% metallic iron to $Fe(OH)_2$. Within the limits of error this represents the same amount of iron obtained by reduction of $Fe(OH)_2$ during the charge process.

* The formulas of the individual compounds denote the actual amount of iron present in this form.

Table 1. Quantitative changes in the phase composition of the iron electrode during the cathodic process

	Fe (%)	*Fe(OH)₂* (%)	*β-FeOOH* (%)	$Q^{möss}$ (mAh)	Q^{g} (mAh)	Δ (%)	*φ* (V)
1	82·0 ± 1·2		18·0 ± 1·2	–	–	–	−0·5
2	80·1 ± 1·5	20·0 ± 1·5	–	12·5 ± 0·9	13·0	3	−1·06
3	91·5 ± 0·8	8·5 ± 0·8	–	15·0 ± 1·0	48·0	–	−1·05

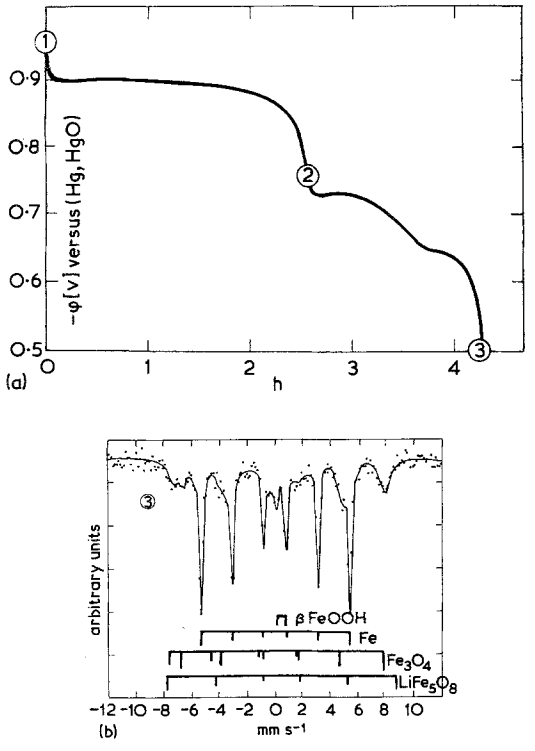

Fig. 6. (a) Discharge curve of an iron electrode recorded after replacing 5 N KOH by 5 N KOH + 9 g l^{-1} LiOH. Discharge current of 7 mA, temperature 30°C; (b) Mössbauer spectrum of the same electrode recorded at point 3 of the discharge curve.

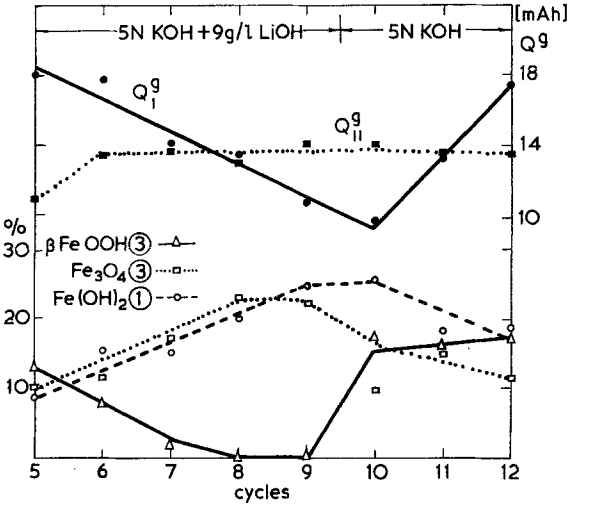

Fig. 7. Change in capacity during the first and second anodic processes during cycling in 5 N KOH + 9 g l^{-1} LiOH. After the ninth cycle the electrolyte was once again replaced by 5 N KOH. The amounts of iron bonded as β-FeOOH and Fe_3O_4 at the end of the discharging (point 3), and as $Fe(OH)_2$ at the beginning of the discharge (point 1) are also shown.

3.2. Effect of LiOH

3.2.1. Anodic process. The addition of lithium hydroxide to the electrolyte of an electrode operating in 5 N KOH brings about qualitative and quantitative changes in the phase composition during the first cycle. Fig. 6 shows a discharge curve and a Mössbauer spectrum recorded at point 3 (− 0·5 V). Fig. 6 illustrates the first cycle after the electrolyte has been changed. The discharge conditions are the same – discharge current 7 mA at 30°C. The spectra recorded at points 1 and 2 do not differ appreciably from those shown in Fig. 2. It is seen, however, that at the end of the second anodic process a new phase appears in addition to β-FeOOH.

Judging from its Mössbauer parameters, this new phase may be identified as magnetite, but since in this case stoichiometry and grain size exert a strong influence, some additional investigations were performed in order to carry out a more rigorous interpretation. It was also taken into account that some authors [12] mentioned the possibility of the formation of inactive lithium ferrates, $LiFeO_2$ and $LiFe_5O_8$. Of all the Mössbauer spectra of lithium ferrates reported in the literature [20, 21], that of $LiFe_5O_8$ is closest to magnetite. Bearing this in mind, the compound

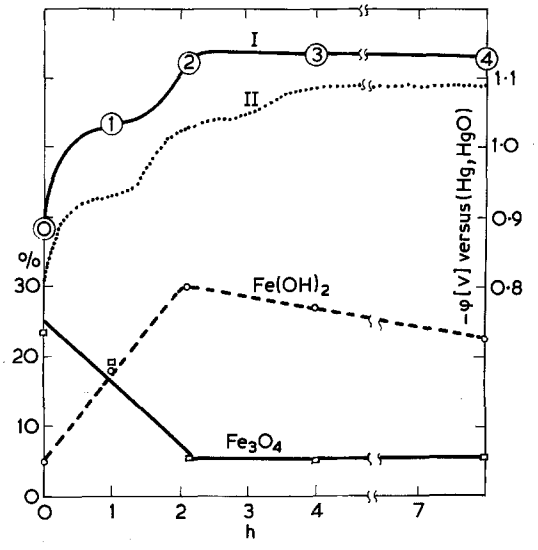

Fig. 8. Change in potential and in the amounts of Fe_3O_4 and $Fe(OH)_2$ during charging of an iron electrode after long operation in 5 N KOH + 9 $g\,l^{-1}$ LiOH (curve I). Charging current 8 mA at a temperature of 20°C. Charging curve II refers to the same electrode after replacing the electrolyte by 5 N KOH.

$LiFe_5O_8$ was synthesized* and its Mössbauer spectrum recorded. Fig. 6 shows its bar diagram. Furthermore, the presence of magnetite was confirmed by the X-ray diffraction pattern of an electrode cycled in lithiated electrolyte.

Further cycling of the electrode leads to a gradual decrease and eventually to the full disappearance of β-FeOOH. During the second anodic step $Fe(OH)_2$ changes to magnetite. This is shown in Fig. 7, which displays the semi-quantitative results of the investigation of an electrode after changing the electrolyte. It is obvious that the decrease of the amount of β-FeOOH and the increase of magnetite leads to a decrease in the capacity of the electrode (Fig. 7).

If the electrolyte is replaced by pure 5 N KOH, formation of β-FeOOH takes place once more in the second anodic process, and there is an increase in capacity. A certain amount of untransformed magnetite still persists (Fig. 7).

3.2.2. Cathodic process. The charging curve of an iron electrode which has operated for a few cycles in an electrolyte containing LiOH up to the full transformation of β-FeOOH into magnetite differs from the curve obtained in pure KOH electrolyte in that the first cathodic process takes place at considerably more negative potentials (Fig. 8, curve 1). Fig. 8 also gives the semi-quantitative results of the determinations of Fe_3O_4 and $Fe(OH)_2$. It is readily seen that during the first cathodic reaction, part of the Fe_3O_4 changes to $Fe(OH)_2$ and that further charging leads to reduction of $Fe(OH)_2$ to metallic iron. At the end of the charge considerable amounts of magnetite and $Fe(OH)_2$ still persist.

If the electrolyte is replaced by pure 5 N KOH and a new charge-discharge cycle is performed, then at the following charging (shown for comparison purposes in Fig. 8, curve II) a new potential arrest may be noticed ($\phi = -0{\cdot}92$ V), possibly due to the transformation of β-FeOOH into $Fe(OH)_2$.

4. Discussion

The study of the electrochemical reactions of the iron electrode in alkaline solutions by means of Mössbauer spectroscopy made it possible to perform a rigorous identification of the reaction products and to follow their quantitative relationships during the process. The relative error of the determinations ranges between 5 and 10%. Such a precision may be considered as satisfactory, taking into account the actual experimental conditions.

It was found that at the end of the charging of the iron electrode in 5 N KOH, untransformed ferrous hydroxide is invariably present in amounts up to 10% besides metallic iron. When operating with LiOH (9–11 $g\,l^{-1}$ LiOH) under identical cycling conditions, unconverted Fe_3O_4 is also present.

At the end of the second anodic process β-FeOOH is always formed when operating in 5 N KOH. Cycling of the electrode up to twenty cycles does not lead to transformation of β-FeOOH into Fe_3O_4 as observed by Silver and Lekas [7] for δ-FeOOH. The same constancy of the reaction product formed during the second anodic process was observed by Teplinskaia *et al.* [5]. However, the compound identified by these authors by means of X-ray diffraction techniques is δ-FeOOH. The presence of β-FeOOH was reported by Labat *et al.* [6] but the lack of quantitative data and the different experimental conditions (working tem-

* The synthesis was performed by firing a stoichiometric mixture of Fe_2O_3 and Li_2CO_3 at 850°C for 1 h. The reaction product was cooled down to room temperature at a rate of 100° h^{-1} [22].

perature) exclude the possibility of any meaningful comparisons.

It is very probable that these differences in the analysed products during the second anodic process are due to some differences in experimental conditions which may prove to be responsible for the direct formation of Fe^{3+} at the electrode surface, as assumed by Armstrong and Baurhoo [24].

When the electrode operates in a lithiated electrolyte, β-FeOOH is gradually transformed into Fe_3O_4. The rate of this transformation depends directly on the lithium content in the electrolyte. This is in accord with the results reported in [7]. The presence of lithium hydroxide also changes the shape of the second anodic step. Indeed, a new potential plateau appears, shifted by 60–80 mV in the negative direction. It is probably due to the transformation of the hydroxide into magnetite (cf. Figs. 2 and 6).

The presence of magnetite is also detected when operating in unlithiated 5 N KOH, but only after repeated overdischarges down to +0·65 V, as observed by other authors [11].

Cycling of an iron electrode in 5 N KOH + 9 $g\,l^{-1}$ LiOH leads to a gradual decrease in capacity (Fig. 7). This contradicts the findings of Hills [15] and of Pyiankova and Yofa [16] according to which there is a considerable increase in capacity when the electrode operates in an electrolyte with 11–15 $g\,l^{-1}$ LiOH. Such a capacity increase was observed in our experiments only during the first cycle after the replacement of the electrolyte when changes in the phase composition had not yet occurred. The increase in capacity is connected with the increased overvoltage of the hydrogen evolution reaction in the presence of minor amounts of lithium in the solution, which has been observed by Hampson *et al.* [23] on a smooth iron electrode.

Further cycling in the presence of LiOH leads to the appearance of a new phase, i.e. of magnetite, which is probably less readily reduced than β-FeOOH. This process competes with the slow hydrogen evolution reaction. This explains why in the subsequent cycling a gradual fall in capacity as well as in increase in the amount of unreduced magnetite at the end of the charge are observed (Figs. 7 and 8). Cycling leads to the establishment of a constant capacity smaller than that obtained prior to replacement of the electrolyte 5 N KOH + LiOH.

The presence of lithium in the electrolyte hinders not only the transformation of magnetite into ferrous hydroxide, but the transformation of the latter into metallic iron as well. Indeed, the amount of this phase at the end of the charge is higher than that found during operation in 5 N KOH (cf. Fig. 6 and Table 1).

The present study showed that the capacity during the first anodic step is due to oxidation of metallic iron obtained by reduction of $Fe(OH)_2$ in the previous cathodic process (Table 1). The electrode formation in 5 N KOH is connected with the appearance of increasing amounts of electrochemically active iron. However, the amount of $Fe(OH)_2$ at the end of the first anodic step remains practically constant. Therefore the charge for the second anodic process (complete transformation of $Fe(OH)_2$ into β-FeOOH) does not change during formation (Fig. 4).

Since at the end of charging a certain amount of untransformed $Fe(OH)_2$ is invariably present, the capacity of the second anodic process is always higher than half the capacity during the first anodic step. This explains the contradiction noted by several authors and casts doubt on Flerov's statement [17] according to which metallic iron could be directly oxidized to the trivalent state.

No trivalent compounds were identified in the potential range between −0·96 and −0·75 V, as assumed by others [13]. The Fe_3O_4 present at the end of the first anodic process during operation in lithiated electrolyte is only the residue of untransformed Fe_3O_4 formed during the previous cathodic process. The increase in its amount takes place between −0·75 and −0·50 V, following the oxidation of $Fe(OH)_2$.

Obviously the present experimental results and considerations deepen the interest toward the phase transformations during the electrochemical processes which take place in iron electrodes in alkaline media. In this respect a detailed study of magnetite would be particularly interesting, for this compound is, in our view, responsible for some of the inconsistencies in the behaviour of the iron electrode.

Acknowledgement

Thanks are due to Professor E. Budevski and Dr R.V. Moshtev for fruitful discussions during the preparation of the manuscript.

References

[1] F. Förster, *Z. Electrochem.* **14** (1908) 295.
[2] O. Faust, *ibid* **13** (1907) 161.
[3] F. Förster and P. Herold, *ibid* **16** (1910) 461.
[4] A.J. Salkind, C.J. Venuto and S.U. Falk, *J. Electrochem. Soc.* **111** (1964) 493.
[5] T.K. Teplinskaya, N.N. Fedorova and S.A. Rozentsveig, *Zh. Fiz. Khim.* **38** (1964) 2176.
[6] J. Labat, J.C. Jarrousseau and J.F. Laurent, 'Power Sources 3', Ed. D.H. Collins, Oriel Press, Newcastle-on-Tyne (1971) 283.
[7] H.G. Silver and E. Lekas, *J. Electrochem. Soc.* **117** (1970) 5.
[8] F. Kukos and V. Makarov, *Sb. Issl. v. oblasti khim. ist. toka, Novocherkask* (1966) 62.
[9] F. Kukos and A. Emez, *Trud. Novocherk. Politekhn. Inst.* **269** (1972) 61.
[10] H. Cnobloch, D. Gröppel, W. Nippe and F.v. Stum, 'Chemie-Ing.-Technik', **45** (1973) 203.
[11] T. Teplinskaya, Z. Shcherbakova and S. Rozentsveig, *Sb. rabot. Khim. ist. toka* **1** (1966) 5.
[12] L.I. Pavlova and V.N. Flerov, *Zh. Prikl, Khim.* **42** (1969) 1407.
[13] V.N. Flerov and L.I. Pavlova, *Electrokhimiya* **3** (1967) 621.
[14] V.N. Flerov, L.I. Pavlova and L.V. Uzinger, *Zh. Prikl. Khim.* **38** (1965) 569.
[15] S. Hills, *J. Electrochem. Soc.* **112** (1965) 1048.
[16] A.P. Pyankova and Z.A. Iofa, *Zh. Prikl. Khim.* **46** (1973) 529.
[17] T. Tomov, T. Ruskov, S. Georgiev, N. Pavlov and R. Kwachkov, Proceedings of the Conf. on Mössbauer Spectrometry, Dresden (1971) 508.
[18] I. Dezci, L. Keszthely, D. Kulgawczuk, B. Molnar and N.A. Eissa, *Phys. Stat. Sol.* **22** (1967) 617.
[19] S. Georgiev, T. Tomov, T. Ruskov, N. Pavlov, *Universalnjie pribori,* **12** (1972) 15.
[20] D.E. Cox, G. Shirane, P.A. Flinn, S.L. Ruby and W.I. Takei, *Phys. Rev.* **132** (1963) 1547.
[21] N. Kelly, V. Follen, M. Hass, W. Shreiner and G. Beard, *ibid* **124** (1961) 80.
[22] J. Remeika and R. Comstock, *J. Appl. Phys.* **35** (1964) 3320.
[23] N.A. Hampson, R.J. Latham and A.N. Oliver, *J. Appl. Electrochem.* **3** (1973) 61.
[24] R.D. Armstrong and I. Baurhoo, *J. Electroanal. Chem.* **40** (1972) 325.